The FEBS Journal

FEBS PRESS science publishing by scientists

Caspase-9 acts as a regulator of necroptotic cell death

Tamás Molnár[1,2], Petra Pallagi[3,4], Bálint Tél[3,4], Róbert Király[5], Eszter Csoma[6], Viktória Jenei[1], Zsófia Varga[1,2], Péter Gogolák[1], Anne Odile Hueber[7], Zoltán Máté[8], Ferenc Erdélyi[8], Gábor Szabó[8], Aladár Pettkó-Szandtner[9], Attila Bácsi[1], László Virág[10], József Maléth[3,4] and Gábor Koncz[1]

1 Department of Immunology, Faculty of Medicine, University of Debrecen, Hungary
2 Doctoral School of Molecular Cellular and Immune Biology, University of Debrecen, Hungary
3 First Department of Medicine, University of Szeged, Szeged, Hungary
4 HAS-USZ Momentum Epithelial Cell Signalling and Secretion Research Group, University of Szeged, Szeged, Hungary
5 Department of Biochemistry and Molecular Biology, Faculty of Medicine, University of Debrecen, Hungary
6 Department of Medical Microbiology, Faculty of Medicine, University of Debrecen, Hungary
7 CNRS, Inserm, iBV, Université Côte d'Azur, Nice, France
8 Medical Gene Technology Unit, Institute of Experimental Medicine, Budapest, Hungary
9 Laboratory of Proteomics Research, Biological Research Centre, Szeged, Hungary
10 Department of Medical Chemistry, Faculty of Medicine, University of Debrecen, Hungary

Keywords
Caspase-9; cell death; inflammation; necroptosis; pancreatitis

Correspondence
G. Koncz, Department of Immunology, Faculty of Medicine, University of Debrecen, 1 Egyetem Square, Debrecen H-4032, Hungary
Tel: +36 52 417 159,
E-mail: konczgb@gmail.com

(Received 22 September 2020, revised 4 March 2021,

doi:10.1111/febs.15898

Necroptosis is a regulated necrotic-like cell death modality which has come into the focus of attention since it is known to contribute to the pathogenesis of many inflammatory and degenerative diseases as well as to tumor regulation. Based on current data, necroptosis serves as a backup mechanism when death receptor-induced apoptosis is inhibited or absent. However, the necroptotic role of the proteins involved in mitochondrial apoptosis has not been investigated. Here, we demonstrated that the stimulation of several death and pattern recognition receptors induced necroptosis under caspase-compromised conditions in wild-type, but not in caspase-9-negative human Jurkat and murine MEF cells. Cerulein-induced pancreatitis was significantly reduced in mice with acinar cell-restricted caspase-9 gene knockout. The absence of caspase-9 led to impaired association of receptor-interacting serine/threonine-protein kinase 1 (RIPK1) and RIPK3 and resulted in decreased phosphorylation of RIP kinases, but the overexpression of RIPK1 or RIPK3 rescued the effect of caspase-9 deficiency. Inhibition of either Aurora kinase A (AURKA) or its known substrate, glycogen synthase kinase 3β (GSK3ß) restored necroptosis sensitivity of caspase-9-deficient cells, indicating an interplay between caspase-9 and AURKA-mediated pathways to regulate necroptosis. Our findings suggest that caspase-9 acts as a newly identified regulator of necroptosis, and thus, caspase-9 provides a promising therapeutic target to manipulate the immunological outcome of cell death.

Abbreviations
AP, acute pancreatitis; AURKA, Aurora kinase A; CHX, cycloheximide; CYLD, cylindromatosis protein; DR, death receptor; GSK3ß, glycogen synthase kinase 3β; HHV-1 or HSV-1, human herpesvirus 1; IBD, inflammatory bowel disease; LPS, lipopolysaccharide; MEF, mouse embryonic fibroblasts; MLKL, mixed lineage kinase domain-like protein; Nec-1, necrostatin-1; NSA, necrosulfonamide; PI, propidium iodide; PRR, pattern recognition receptor; RIPK1, receptor-interacting serine/threonine-protein kinase 1; TNF-α, tumor necrosis factor-α; TRAIL, tumor necrosis factor-related apoptosis-inducing ligand.

Introduction

In the past few years, novel cell death pathways have been discovered and classified and these cell death modalities have been shown to differently affect the activation of immune responses [1,2]. In addition to intensity, the immunological outcome of cell death also has fundamental impact on the evolution of various inflammatory diseases, autoimmune processes, degenerative disorders, and immune surveillance of tumors. The molecular programs that govern switches between the different modes of cell death remain obscure despite the enormous potential of putative therapeutic applications.

Apoptosis is mediated by both intrinsic and extrinsic pathways. The extrinsic pathway is induced by cell death receptors (DR) interacting with their specific ligands such as tumor necrosis factor-α (TNFα), Fas ligand and tumor necrosis factor-related apoptosis-inducing ligand (TRAIL) [3,4]. These interactions lead to the recruitment of the adaptor protein FAS-associated death domain, which activates apoptosis initiator enzymes caspase-8 and caspase-10, resulting in the activation of effector caspases (type I cells), or initiation of the mitochondrial apoptotic pathway (type II cells) [5,6]. The intrinsic pathway can be activated by various stimuli which induce mitochondrial membrane permeabilization [7]. Cytochrome c released from the mitochondria interacts with the apoptotic protease-activating factor 1, which recruits caspase-9 [8]. The resulting molecular complex forms the apoptosome, which maintains caspase-9 in an active conformation resulting in the activation of effector caspases [9,10].

Cell death is controlled by multiple interconnected pathways, among them necroptosis, a highly regulated necrosis-like cell death mode [11–13]. Necroptosis utilizes a unique signaling pathway requiring the involvement of receptor-interacting serine/threonine-protein kinases 1 and 3 (RIPK1 and RIPK3) [2,14] and mixed lineage kinase domain-like protein (MLKL) [15]. Upon stimulation of DRs, necroptosis requires inhibited caspase activity because active caspase-8 blocks necroptotic signaling [2,16] primarily through the cleavage of RIPK1 [17], RIPK3 [18,19], and cylindromatosis protein (CYLD) [20] which acts as the deubiquitinase enzyme of RIPK1. Even though the crucial role of DR-mediated apoptosis in the negative regulation of necroptosis is investigated extensively, the function of caspase-9 in necroptosis has not been documented yet.

Perturbations in necroptotic signaling contribute to the pathogenesis of many diseases [21]. Upregulated necroptosis occurs in retinal disorders, neurodegenerative diseases, and ischemia reperfusion [22]. Downregulation of necroptosis contributes to infectious diseases, carcinogenesis, or the resistance to anti-cancer treatments [23]. Dysregulation of the balance between apoptosis and necroptosis plays a crucial role in inflammatory diseases such as inflammatory bowel disease (IBD), pancreatitis, acute kidney injury, hepatitis, and various skin disorders [21,24].

More than 70 human molecules have been documented as regulators of necroptotic events along the RIPK1-RIPK3-MLKL axis [21]. Among them Aurora kinase A (AURKA) has recently been identified as a binding partner of RIPK3 [25–28] and an inhibitor against unwanted necroptosis. AURKA, with its downstream partner, GSK3β regulates the formation of RIPK1-RIPK3 complex [25]. Silencing or blocking AURKA or GSK3β leads to spontaneous necroptosis [25].

In the present study, we report that caspase-9 is required for death and pattern recognition receptor (PRR)-induced necroptosis *in vitro* and increases the severity of cerulein-induced pancreatitis *in vivo*, even though caspase activity is inhibited under necroptotic conditions. We provide evidence that caspase-9 regulates the formation of the necrosome. Our results may offer novel strategies for regulating necroptosis through targeting caspase-9 and provide relevant information on the cross-talk of stress-induced apoptosis and programmed necrosis.

Results

Caspase-9 plays a role in death receptor-mediated necroptosis

It is well known that DR-mediated apoptosis dominates necroptosis [2,13], but the link between necroptosis and intrinsic apoptosis has not been studied in detail [21–24]. Several substrates of caspase-8 have been documented as critical regulators of necroptosis, such as RIPK1, RIPK3, and CYLD [20]; however, its most well-known substrates, the downstream caspases, have been only marginally studied during necroptosis. Silencing of caspase-3 and caspase-7 did not influence TNF-induced necroptosis [29], while the effect of caspase-9 on necroptosis has not yet been investigated.

To assess this, we induced cell death in JA3 Jurkat cells and in their caspase-9-negative subclone (JA3-C9). Cells were treated with the classical necroptosis inducing cocktail of TNF, SMAC mimetic (BV6), and pan-caspase inhibitor Z-VAD (TBZ) [30,31] or caspase-8 inhibitor Q-IETD-Oph [32]. In the culture of caspase-9-deficient cells, the rate of cell death was

significantly lower compared with that of caspase-9-positive ones (Fig. 1A). We used a necroptosis inhibitor, necrostatin-1 (Nec-1), and validated that it successfully blocked TBZ-induced cell death. To confirm that the observed cell death is strictly caspase-9 dependent, we retransfected the JA3-C9 subclone with wild-type caspase-9. Reconstitution of caspase-9 expression restored the sensitivity of transfected cells (JA3-C9 retr) to TBZ-induced necroptosis (Fig. 1A).

To verify the essential role of caspase-9 in the necroptotic signaling of other DRs, we triggered necroptosis with recombinant FasL or TRAIL in the presence of BV6 and Z-VAD (FBZ or TrBZ, respectively). Treatment with either FasL or TRAIL activated necroptosis only in the wild-type cells, whereas in the absence of caspase-9 significantly alleviated necroptosis was detected in both cases. Retransfection of caspase-9 into JA3-C9 cells also restored the intensity of cell death after these stimuli (Fig. 1B,C). Jurkat cells were also cocultured with FasL-overexpressing human B-cell line (WSU-FasL) in the presence of Z-VAD, because this stimulus was able to induce necroptosis without the synergic effect of BV6. Significantly decreased necroptosis was detected in caspase-9-deficient cells compared with wild-type cells upon WSU-FasL induction (Fig. 1D). In these Jurkat cells, the same expression level of the most widely studied necroptosis regulatory molecules (RIPK1, RIPK3, MLKL, caspase-8, CYLD, TAK1) was detected regardless of the presence of caspase-9 (Fig. 1E). We also checked the intensity of necroptosis under caspase-8 compromised conditions. For this, wild-type and caspase-9-deficient Jurkat cells were treated with a specific caspase-8 inhibitor (Q-IETD-Oph) in combination with BV6 and TNF-α. Following this treatment, the intensity of necroptosis and its caspase-9 dependence was comparable to TBZ-induced cell death (Fig. 1F).

To study whether caspase-9 acts on necroptosis only or controls necrosis in general, we treated the cells

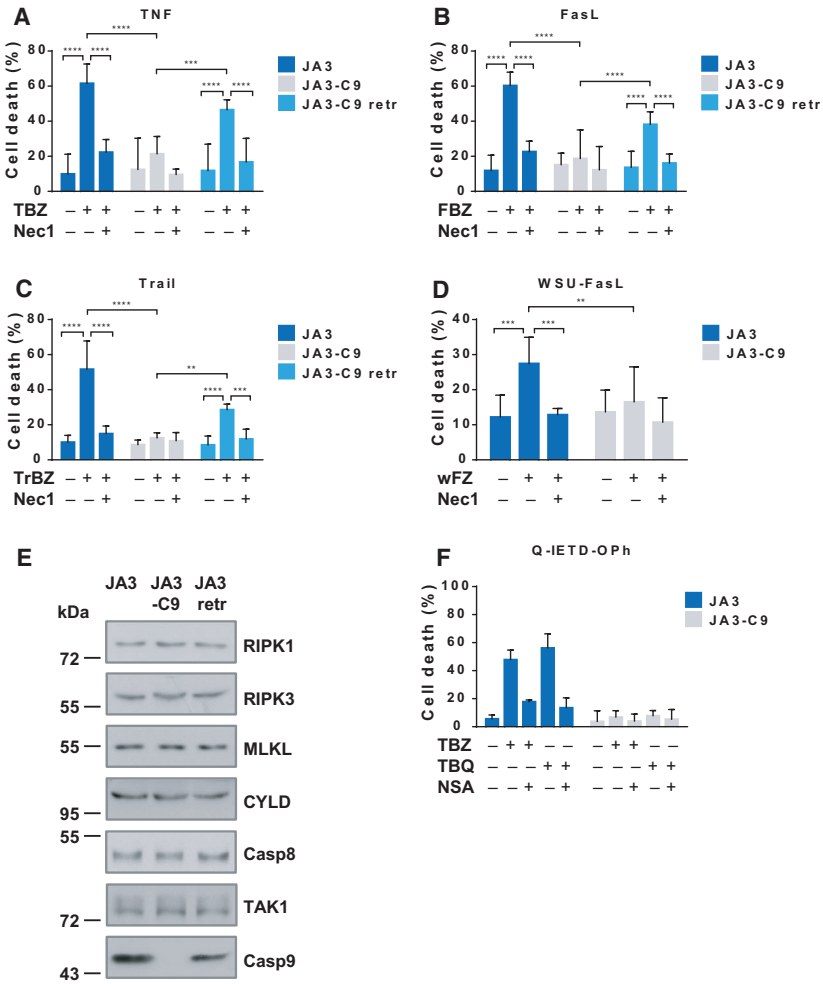

Fig. 1. Caspase-9 plays a role in DR - mediated necroptosis. (A) JA3 cells, its caspase-9-deficient counterpart (JA3-C9), and JA3-C9 cells retransfected with caspase-9 (JA3-C9 retr) were pretreated with 10 μM Z-VAD, 40 μM Nec-1, and 1 μM BV6 for 1 h and activated with 50 ng·mL^{-1} recombinant human TNF-α, (B) 30 ng·mL^{-1} flag-tagged recombinant FasL or (C) 40 ng·mL^{-1} flag-tagged recombinant Trail cross-linked with the anti-flag (M2) antibody. After 24 h, cell death was determined by PI staining. (D) JA3 and JA3-C9 cells were pretreated with 10 μM Z-VAD and cocultured with cell tracker green-stained human FasL expressing WSU B-cell line (wF) at a ratio of 1 : 5. After 24 h, the extent of cell death was determined by PI staining in the cell tracker-negative population. (E) The expression of the indicated molecules was determined by western blotting of total cell lysates. Representative images of three independent experiments are shown. (F) JA3 and JA3-C9 cells were pretreated with 10 μM Z-VAD, 10 μM Q-IETD-OPh, 1 μM BV6, and 1 μM NSA for 1 h and activated with 50 ng·mL^{-1} human TNFα. After 24 h, cell death was determined by PI staining. Figure A-D, F shows the mean plus SD of at least three independent experiments. Significance is indicated by $^{**}P < 0.01$; $^{***}P < 0.005$; $^{****}P < 0.001$.

with ionomycin and observed that the intensity of ionomycin-induced necrosis was comparable in both JA3 and JA3-C9 cells (Fig. 2A). Treatment with H_2O_2 has been shown to induce both apoptosis and classical necrosis in Jurkat cells [33]. The role of caspase-9 is well-known in stress-induced apoptosis, and consequently, H_2O_2 induces apoptosis only in caspase-9-positive cells, but in the presence of Z-VAD, H_2O_2 treatment resulted in equally intense necrosis in both JA3 and JA3-C9 cells (Fig. 2B).

In addition to RIPK1-mediated necroptosis, RIPK1-dependent apoptosis has also been documented, primarily in the presence of SMAC mimetics under conditions that allow caspase activation [34]. JA3 and its caspase-9-negative subclone were stimulated with TNF and BV6, and the activity of effector caspases was investigated. In accordance with published results [35], the absence of caspase-9 did not modify the intensity of RIPK1-mediated apoptosis (Fig. 2C,D). Our results indicate that in addition to its well-known role in intrinsic apoptosis, caspase-9 is specifically required for necroptosis, whereas it has no role in necrosis or in RIPK1-mediated apoptosis.

Caspase-9 is associated with RIPK3 upon necroptotic stimulus

Considering that DR-induced necroptosis takes place at caspase-compromised conditions, the protease activity of caspase-9 is not required for its role in the signaling. Therefore, we assumed that caspase-9 contributes to necroptosis as an adaptor protein. We checked the molecules recruited to caspase-9, in particular, its association with RIPK1, RIPK3, and MLKL.

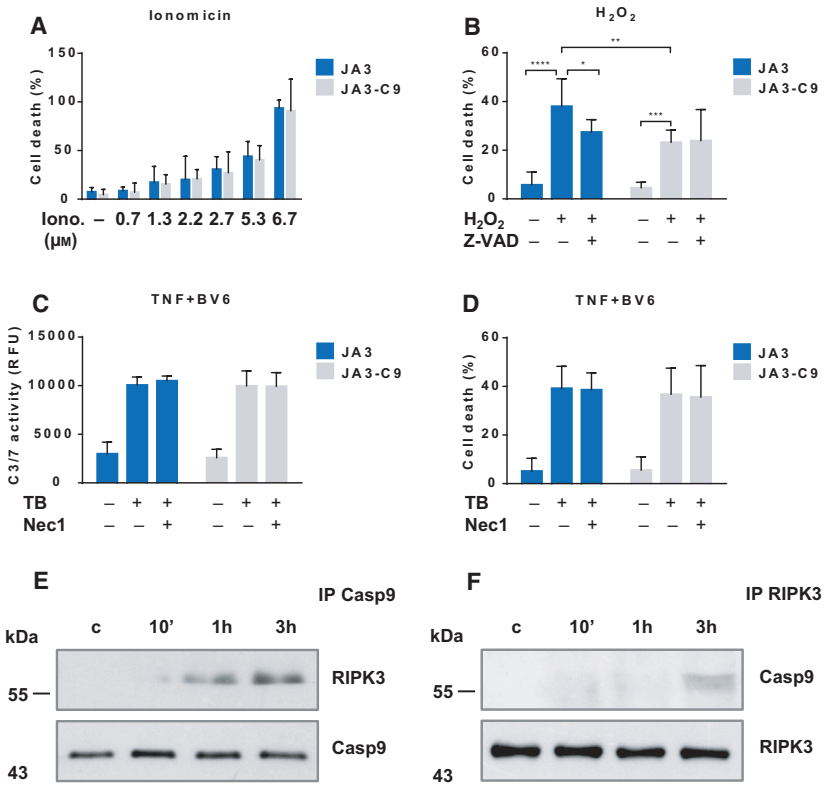

Fig. 2. Caspase-9 interacts with RIPK3 during necroptosis. (A) JA3 and JA3-C9 cells were treated with the indicated doses of ionomycin or (B) pretreated with 10 μM Z-VAD for 1 h and activated with 400 μM H_2O_2. The degree of total cell death was quantified based on the uptake of PI. (C-D) JA3 and JA3-C9 cells were pretreated with 40 μM Nec-1 and 1 μM BV6 for 1 h followed by stimulation with 50 ng·mL^{-1} TNF. (C) Caspase-3/7 activity, expressed as relative fluorescence units (RFU), was measured 30 min after the addition of the profluorescent substrate Z-DEVD-R11. (D) The degree of total cell death was determined by PI staining. Panels A-D show the mean plus SD of at least three independent experiments. Significance is indicated by *$P < 0.05$; **$P < 0.01$; ***$P < 0.005$; ****$P < 0.001$. (E) JA3 and JA3-C9 cells were pretreated with 10 μM Z-VAD and 1 μM BV6 for 1 h and activated for the indicated times with 50 ng·mL^{-1} human TNF-α. Following immunoprecipitation from total cell lysates with anti-caspase-9 or (F) anti-RIPK3, the recruited molecules were detected by western blotting. Figures E and F shows representative images of three independent experiments.

We were unable to detect any interaction between caspase-9 and RIPK1 or MLKL, but we observed a weak and transient association of RIPK3 with caspase-9, which peaked at 3 h after initiation of necroptosis (Fig. 2E). Immunoprecipitation with anti-RIPK3 Ab has confirmed RIPK3-caspase-9 association (Fig. 2F). According to our data, caspase-9 can be considered as a regulator of necroptosis that interacts faintly with RIPK3.

Caspase-9 regulates death- and PRR-mediated necroptosis in MEF cells

Necroptosis has been published to highly depend on the cell type and on the sorts of stimuli. To determine whether the role of caspase-9 in necroptosis is a general requirement or specific to the Jurkat cells, we studied the necroptotic sensitivity of caspase-9-deficient MEF cells (MEF-C9) and their wild-type counterparts. Similarly to our observations in Jurkat cells, TBZ activation induced necroptosis in wild-type, but not in the caspase-9-deficient MEFs (Fig. 3A). We also stimulated necroptosis with FasL and found that MEF-C9 cells were less susceptible to FBZ-induced necroptosis than wild-type MEFs (Fig. 3B). These cells are also sensitive to TNF, Z-VAD, and cycloheximide (CHX)-triggered (TCZ) necroptosis; thus, this treatment induced intense necroptosis in MEFs, while caspase-9-deficient cells were less sensitive to these stimuli (Fig. 3C). All these results confirm that caspase-9 contributes to necroptosis, and provide evidence that its role is essential for necroptosis in both human and mouse cells.

Necroptosis has been observed not only after DR-mediated signals, but also as a result of various other stimuli, among them PRR activation has been investigated the most intensely [36]. Wild-type and caspase-9-negative MEF cells were treated with lipopolysaccharide (LPS) in the presence of Z-VAD. Similar to the results detected after DR activation, in the culture of caspase-9-deficient cells significantly fewer dead cells were detected after LPS exposure compared with that of wild-type cells (Fig. 3D). Mouse cells have been published to be sensitive to human herpesvirus 1 (HHV-1 or HSV-1)-induced necroptosis [37]. MEF and MEF-C9 cells were infected with HSV-1 in the presence of Z-VAD, and it was observed that the lack of caspase-9 protected MEF cells from HSV-1-induced necroptosis (Fig. 3E). We also checked the expression of the main necroptosis regulatory molecules (RIPK1, RIPK3, MLKL, caspase-8, CYLD, TAK1), and it was comparable in both wild-type and caspase-9-deficient MEF cells (Fig. 3F). Our results indicate that caspase-9 plays a general role in necroptosis, as caspase-9 deficiency prevents necroptosis in both human and murine cells under various stimuli.

Caspase-9 regulates upstream events of necroptotic signaling

To dissect the role of caspase-9 in the molecular background of necroptosis, we examined the phosphorylation of the core components of the necroptotic pathway. RIPK1 phosphorylation (S166) was strongly elevated in JA3 cells following TBZ activation, but only marginal phosphorylation of RIPK1 was found in JA3-C9 cells (Fig. 4A). Similarly, more intense RIPK3 phosphorylation (S227) was detected in wild-type, than in JA3-C9 cells 6 h postactivation (Fig. 4A). We compared the association of RIPK1 with RIPK3 in the presence and absence of caspase-9 to analyze the regulated events in the course of the necroptotic process. We detected the RIPK1/RIPK3 interaction by immunoprecipitation 3–6 h following TBZ activation in wild-type Jurkat cells, but we could not observe this association in the absence of caspase-9 (Fig. 4B,C). The failure of RIPK1/RIPK3 interaction in JA3-C9 cells indicates that caspase-9 regulates the upstream events of necroptotic signaling.

We overexpressed RIPK1 and RIPK3 assisted by a Tet-On inducible system in both JA3 and JA3-C9 cells to verify the regulation of the necrosome assembly by caspase-9. Overexpression of either RIPK1 or RIPK3 reconstituted the sensitivity of JA3-C9 cells to TBZ-induced necroptosis (Fig. 4D-G). These results demonstrate that the downstream parts of the necroptotic pathway still function normally in the absence of caspase-9 in both RIPK1- and RIPK3-overexpressing cells.

AURKA inhibitor restores the sensitivity of caspase-9-deficient cells to TNF-induced necroptosis

We have shown that caspase-9 regulates the initial phase of necroptotic signaling. Caspase-9 interacts weakly with the basic components of necroptotic signaling pathway; therefore, we hypothesized that it acts primarily on molecules that regulate the assembly of the necrosome. AURKA has been identified recently as an interaction partner of RIPK3 and RIPK1 [25,26]. We tested the association of caspase-9 with AURKA under necroptotic conditions in Jurkat cells and found that AURKA was associated with caspase-9 in a stimulus-dependent manner (Fig. 5A,B). AURKA and its downstream target, GSK3β, have been published to downregulate necroptosis. We tested the TBZ-induced necroptosis in the presence of AURKA inhibitor (CCT137690) or GSK3β inhibitor (AR-A014418) in JA3 and JA3-C9 cells. Low doses of

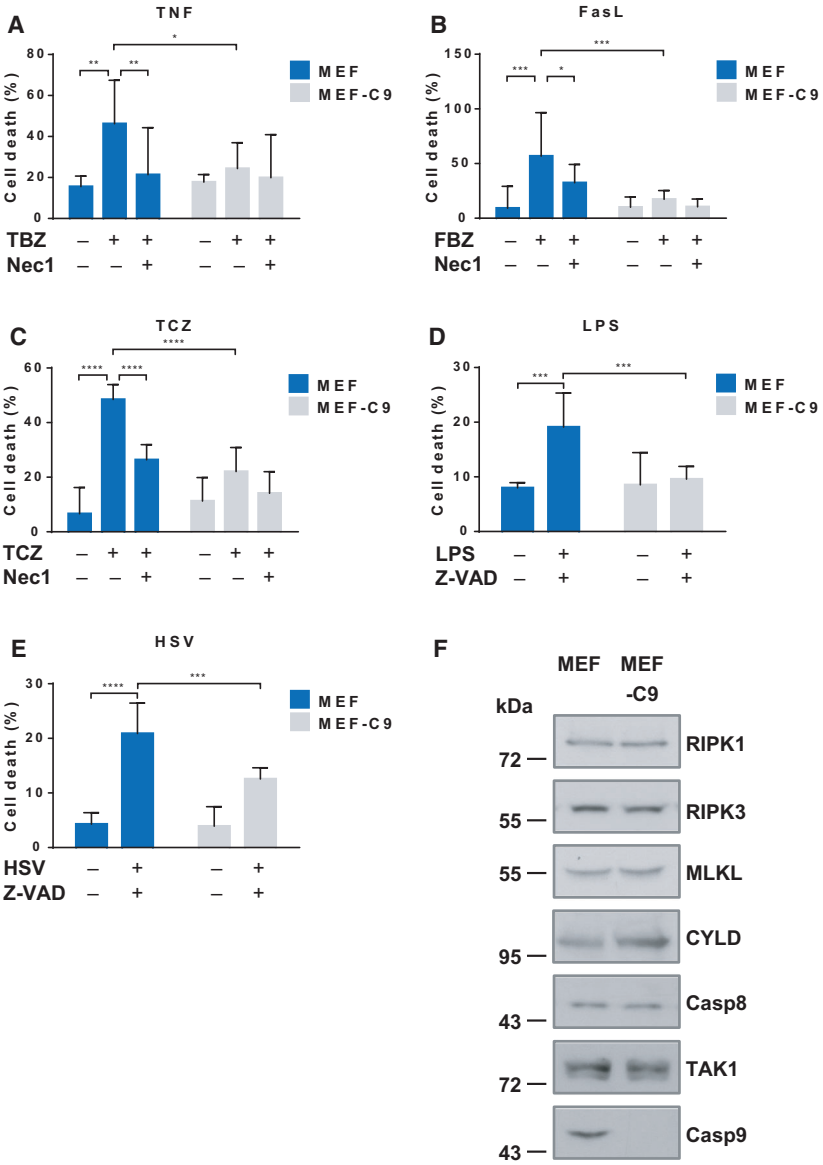

Fig. 3. Caspase-9 regulates death- and PRR-mediated necroptosis in MEF cells. (A) MEF and their caspase-9-deficient counterpart (MEF-C9) were pretreated with 10 μM Z-VAD, 40 μM Nec-1, and 1 μM BV6 for 1 h and activated with 20 ng·mL^{-1} human TNF-α or (B) 40 ng·mL^{-1} flag-tagged recombinant FasL. After 24 h, cell death was determined by PI staining. (C) MEF and MEF-C9 cells were pretreated 10 μM Z-VAD, 40 μM Nec-1, and 0.4 μg·mL^{-1} CHX for 1 h and activated with 20 ng·mL^{-1} human TNFα. After 24 h, cell death was determined by PI staining. (D) MEF and MEF-C9 cells were pretreated 50 μM Z-VAD for 1 h and were activated with 100 ng·mL^{-1} LPS or (E) were infected with HHV-1 at MOI 5. After 24 h, cell death was determined by PI staining. Panels A-E show the mean plus SD of at least three independent experiments. Significance is indicated by $*P < 0.05$; $**P < 0.01$; $***P < 0.005$; $****P < 0.001$. (F) The expression of the indicated molecules was visualized by western blotting of total cell lysates. Representative images of three independent experiments are shown.

CCT137690 (< 2.5 μM) or AR-A014418 (<20 μM) had only minimal effects on the cell survival; however, higher doses of CCT137690 (≥ 2.5 μM) and AR-A014418 (≥ 20 μM) elevated the ratio of dead cells (Fig. 5C-F). Cotreatment with low doses of either CCT137690 or AR-A014418 with TBZ increased necroptosis, and this cell death was effectively blocked by all of the applied necroptosis inhibitors/necrostatin-1, GSK'872, and necrosulfonamide (NSA)/ (Fig. 5G,H). Importantly, cotreatment of either CCT137690 or AR-A014418 with TBZ restored the necroptosis sensitivity of the caspase-9-deficient cells.

Caspase-9-mediated regulation of AURKA was confirmed by the investigation of AURKA phosphorylation. AURKA phosphorylation on T288 was observed only in JA3 but not in JA3-C9 cells, and this phosphorylation was increased upon TBZ stimuli indicating that the activity of this kinase is regulated by caspase-9 (Fig. 5I). In summary, caspase-9 and the AURKA-GSK3β pathways interact in the regulation of necroptosis in a still unidentified way.

Knockout of caspase-9 in pancreatic acinar cells decreases the severity of cerulein-induced acute pancreatitis

To confirm the role of caspase-9 in necroptosis *in vivo*, we compared the severity of cerulein-induced experimental acute pancreatitis (AP) in wild-type and pancreas acinus-specific caspase-9 knockout mice.

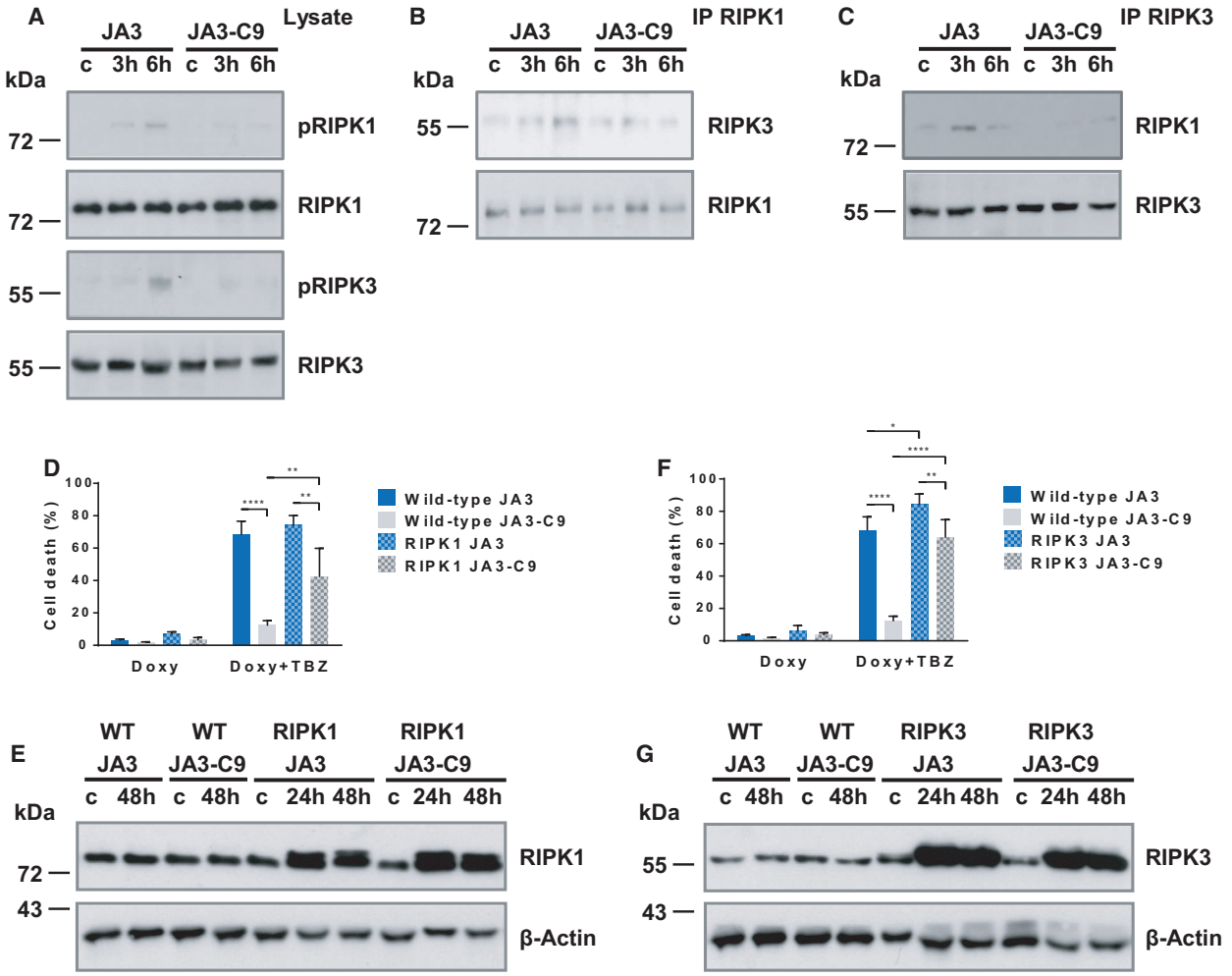

Fig. 4. Caspase-9 regulates the assembly of necrosome during necroptosis. (A) JA3 and JA3-C9 cells were pretreated with 10 μM Z-VAD and 1 μM BV6 for 1 h and activated for the indicated times with 50 ng·mL^{-1} human TNF-α. Phosphorylation of RIPK1 (S166) and RIPK3 (S227) was detected from total cell lysates. (B) Following immunoprecipitation from total cell lysates with anti-RIPK1 or (C) anti-RIPK3 antibodies, the recruited molecules were detected by western blotting. (D) RIPK1 or (F) RIPK3 overexpression was activated with 2 μg·mL^{-1} doxycycline for 24 h, and cells were pretreated with 10 μM Z-VAD and 1 μM BV6 and activated with 50 ng·mL^{-1} human TNF-α. Cell death was determined by PI uptake, 24 h after TNF activation. Data are presented as the mean plus SD of three independent experiments. Significance is indicated by $*P < 0.05$; $**P < 0.01$; $****P < 0.001$. (E) Cells were pretreated with 2 μg·mL^{-1} doxycyclin for the indicated times, and the expression of RIPK1 or (G) RIPK3 was detected from total cell lysates by western blotting. Figure A-C, E, G is representative images of three independent experiments.

Pancreas acinus-specific knockout was achieved by crossing of caspase-9 LoxP animals with pancreatic acinar cell-specific-cre mice expressing tamoxifen-inducible Cre recombinase under the direction of the Cela1 promoter (Fig. 6A,B). Caspase-9 knockout was confirmed by immunostaining (Fig. 6C). In this experiment, mice were i.p. injected hourly (eight times) with either physiological saline (control) or 50 μg/bwkg cerulein to induce AP. Overall, in this experimental model we observed a remarkable improvement of pancreatitis severity in the caspase-9 knockout animals. The control mice had normal pancreatic histology in both groups, whereas cerulein hyperstimulation caused pancreatic damage as demonstrated in Fig. 7A. Importantly, knockout of caspase-9 in pancreatic acinar cells significantly decreased the histological scores and improved serum amylase activity. The extent of interstitial edema (2.5 ± 0.14 for WT vs 1.38 ± 0.28 for KO) and leukocyte infiltration (2.68 ± 0.15 for WT vs 1.38 ± 0.26 for KO) was significantly improved, and the extent of necrosis was completely restored to the control level (14.25 ± 0.27 for WT vs 1.71 ± 0.75 for

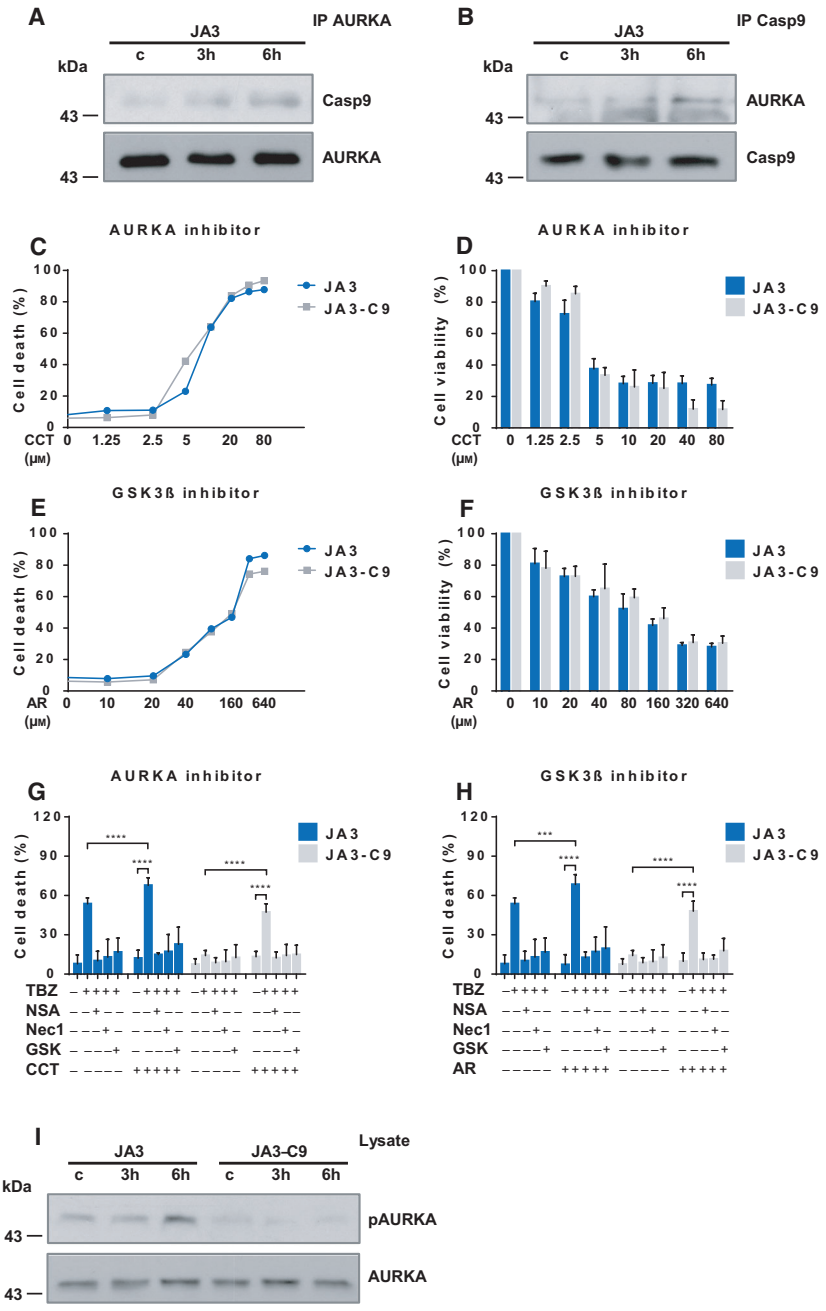

Fig. 5. Aurora kinase A inhibitor restores TNF/BV6/Z-VAD-induced cell death in caspase-9-deficient Jurkat cells. (A) JA3 and JA3-C9 cells were pretreated with 10 μM Z-VAD and 1 μM BV6 for 1 h and activated for the indicated times with 50 ng·mL^{-1} human TNF-α. Following immunoprecipitation with anti-AURKA or (B) anti-caspase-9, the recruited molecules were detected by western blotting. Figure A and B shows a representative image of three independent experiments. (C, D) JA3 and JA3-C9 cells were treated with the indicated doses of CCT137690 (AURKA inhibitor) or (E, F) AR-A014418 (GSK3β) inhibitor 24 h. (C, E) The extent of cell death was determined by PI staining. (D, F) Cell cytotoxicity was measured with Cell Counting Kit-8, and cell viability (%) was expressed as a percentage relative to the untreated control cells. (G) JA3 and JA3-C9 cells were pretreated with 2.5 μM CCT137690 (AURKA inhibitor) or (H) 20 μM AR-A014418 (GSK3β inhibitor) in combination with 10 μM Z-VAD, 1 μM BV6, 1 μM NSA, 40 μM Nec-1, and 7.5 μM GSK'872 for 1 h followed by activation with 50 ng·mL^{-1} human TNF-α. After 24 h, the extent of cell death was determined by PI staining. Panels C-H show the mean plus SD of at least three independent experiments.Significance is indicated by ***$P < 0.005$; ****$P < 0.001$. (I) Phosphorylation of AURKA (T288) was detected from total cell lysates by western blotting. Representative images of three independent experiments are shown.

KO) (Fig. 7B-E). To demonstrate that cerulein-induced necrosis occurred due to necroptosis, we examined the phosphorylation of necrosome components. We detected increased RIPK1 and RIPK3 phosphorylation in pancreatic tissue samples following cerulein treatments in wild-type mice, but not in caspase-9-deficient animals (Fig. 7F,G).

These results highlight the major role of caspase-9-mediated necroptosis in the development of experimental AP.

Discussion

Switching between cell death modalities may have paramount importance to avoid unwanted inflammatory outcome of cell death in various diseases such as retinal disorders, neurodegenerative diseases, ischemia reperfusion, and inflammatory disorders such as IBD, pancreatitis, and hepatitis [22]. The mechanisms executing various cell death processes may be interconnected more strictly than previously thought [38].

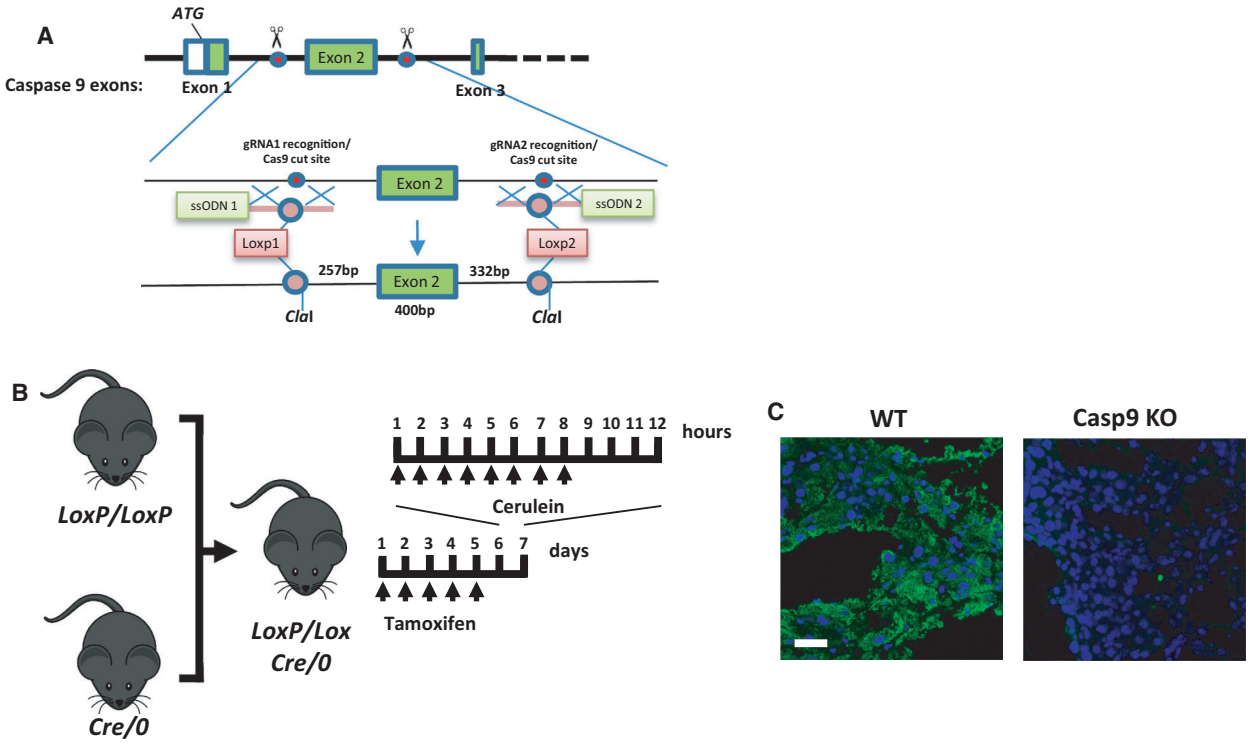

Fig. 6. Pancreatic acinar cell-specific deletion of caspase-9. (A) The gene modification strategy for generating the caspase-9 floxed animals. (B) Schematic representation of the cerulein-induced AP experimental protocol. (C) Immunostaining of caspase-9 in pancreatic acinar cells. Scale bar: 100 μm.

Caspase-9 has been discovered as the initiator caspase of the mitochondrial apoptotic pathway, but its role in both nonapoptotic cell death processes [39,40] and in autophagy has also been documented [41,42]. FasL plus caspase inhibitor [43] or cytotoxic T cell-induced necrotic cell death [44] were also reduced in caspase-9-deficient cell lines. Here, we have shown that necroptosis is blocked in the absence of caspase-9. These results have been confirmed in different cell lines of human and murine origin upon stimulation of all DRs, PRRs, and HSV1 infection. In all these experiments, necroptosis was induced under caspase-compromised conditions which indicate that caspase-9 acts as an adaptor protein in necroptotic signaling. In accordance with this scenario, previous studies have demonstrated that pharmacological inhibition of caspase-9 did not modify necroptosis intensity [45,46].

It is reasonable to assume that the common molecules of different cell death signals regulate the transition for one cell death form to another, and thus, caspase-9 poses an attractive target for pharmacological interventions. We checked the role of caspase-9 in one of the most intensely studied inflammatory disorders, AP. Necroptosis inhibitors, as well as RIPK3 [14] or MLKL [47] deficiency, have been published to block AP, but caspase inhibitors remain ineffective in *in vivo* pancreatitis models [48]. Consistent with the demonstrated role of caspase-9 in *in vitro* experiments, we presented here that acinar cell-specific depletion of caspase-9 protected mice from cerulein-induced AP. Necroptosis is considered as a backup mechanism of apoptosis, because the absence of caspase-8 or caspase inhibition activates necroptosis. We can assume that preventing one type of regulated cell death induces the activation of an alternative cell death pathway to compensate the failure. In accordance with this hypothesis, decreased apoptosis markedly stimulated necrosis in pancreatitis model [49]. Surprisingly, our data indicate that the intensity of necroptosis was reduced or even ceased in the absence of caspase-9 both in *in vitro* and *in vivo* experimental settings. Our results suggest that caspase-9 is also involved in the signaling of two different cell death pathways. It is reasonable to assume that it may play a role in the cross-regulation of apoptosis and necroptosis, and further studies should be performed to study its contribution to inflammatory disorders.

The *in vivo* appearance of necroptosis indicates that in addition to caspase-mediated processes, various regulatory mechanisms control necroptosis that are independent of caspase activity [21]. The expression, the

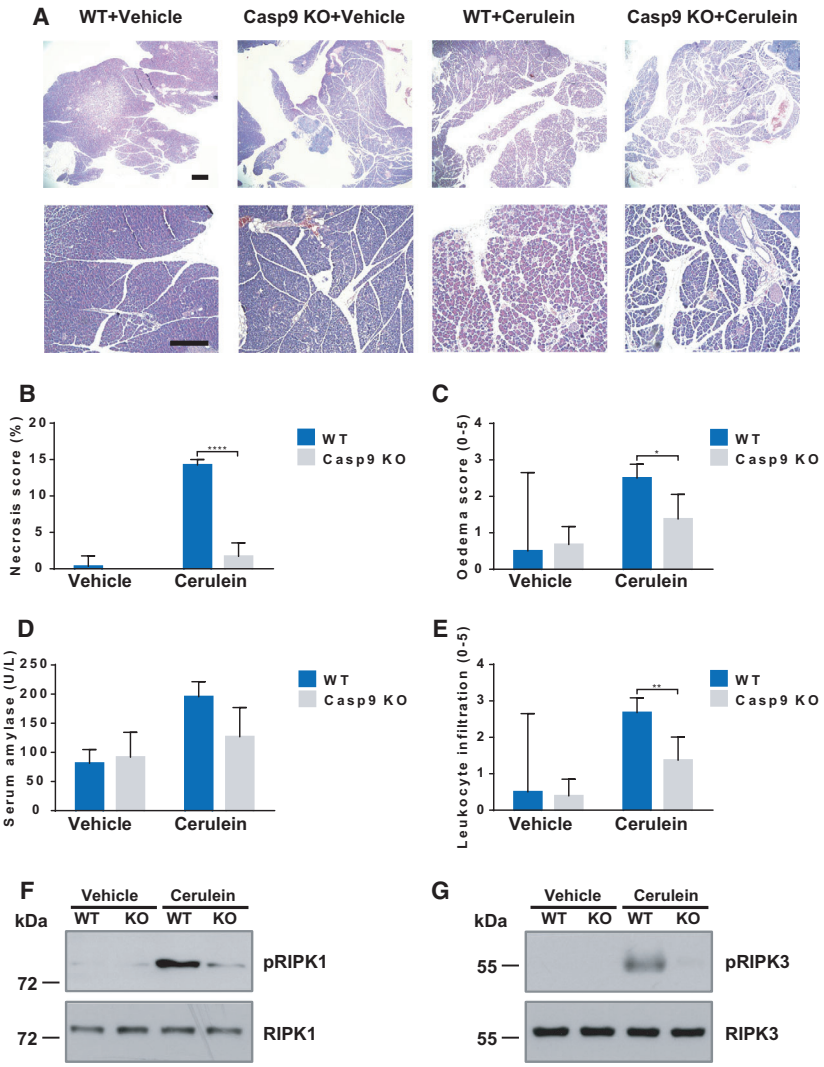

Fig. 7. Knockout of caspase-9 in pancreatic acinar cells decreases the severity of cerulein-induced AP. (A) Representative images of pancreatic histology in cerulein-induced pancreatitis. WT and mice with pancreatic acinar cell-restricted caspase-9 gene inactivation were given eight hourly i.p. injections of either physiological saline (vehicle groups) or 50 μg/bwkg cerulein. Scale bar: 100 μm. (B-E) Histological scores for edema, inflammatory cell infiltration, % of the total area for necrosis, and serum amylase activity were evaluated (n = 6–8 mice per group). Panels B-E show the mean plus SD of three independent experiments. (F-G) Phosphorylation of RIPK1 (S166) and RIPK3 (Thr231/Ser232) was detected from total cell lysates isolated from whole pancreatic tissue. WT refers to *LoxP/LoxP* animals, the vehicle group received sunflower oil only. Significance is indicated by *P < 0.05; **P < 0.01; ****P < 0.001.

interaction partners, the posttranslational modifications, and the localization of necrosome components are tightly regulated to control necroptosis [21]. We demonstrated that the expression levels of RIPK1 and RIPK3 did not depend on caspase-9, but it was required for optimal RIPK1/RIPK3 association. We also identified caspase-9 as a new binding partner of RIPK3. The phosphorylation of RIPK1 and RIPK3 decreased in the absence of caspase-9. It is important to note that although RIPK1 initiates RIPK3 activation during DR -driven necroptosis, it inhibits the activation of RIPK3 in PRR-induced necroptosis [50]. We assume that caspase-9 may act more on RIPK3. This process can consequently controls RIPK1 phosphorylation in DR-induced necroptosis because the stability of the necrosome has been reported to regulate the phosphorylation of both RIPK1 and RIPK3 [51]. The phosphorylation of at least one interaction partner of RIPK3, namely of AURKA, was also dependent on caspase-9 during necroptosis. We revealed that AURKA was associated with caspase-9 upon TBZ stimulus, but further investigations are needed to determine the exact molecular background of caspase-9 and AURKA interaction.

RIPK3 dimerization is the most critical points of necroptosis induction, and increased expression of RIPK3 can induce its oligomerization and can initiate necroptosis [52,53]. We have shown that overexpression of RIPK1 and RIPK3 restores the necroptosis sensitivity of caspase-9-deficient cells and can bypass caspase-9-mediated regulation of necroptosis. It has been published that AURKA-GSK3ß axis downregulates necrosome formation [25]. Inhibition of either AURKA or its downstream substrate, GSK3ß, restored necroptosis sensitivity of caspase-9-deficient cells as did the overexpression of necrosome

components. Altogether, our results indicate that caspase-9 acts as a newly identified regulator in the fine-tuning of necroptotic signaling, and can control the cross-regulation of intrinsic apoptosis and necroptosis.

Materials and methods

Reagents

The following commercial reagents were used in this study: Z-VAD (ApexBio, Houston, TX, USA; #A1902), Q-IETD-Oph (BioVision, Milpitas, CA, USA; #1176), cycloheximide (Sigma-Aldrich, St. Louis, MO, USA; #C6255), necrostatin-1 (Abcam, Cambridge, UK; #ab141053), necrosulfonamide (Tocris Bioscience, Bristol, UK; #5025), CCT137690 (ApexBio; #A4132), AR-A014418 (Selleck Chemicals, Houston, TX, USA; #S7435), TNF-α (BioLegend, San Diego, CA, USA; #570104), FasL (Enzo Life Sciences, Farmingdale, NY, USA; #ALX-522-001-C010), trail (Enzo Life Sciences; #ALX-522-003-C010), ionomycin (Sigma-Aldrich; #I0634), H_2O_2 (Sigma-Aldrich; #H1009), LPS (Sigma-Aldrich; #L8643), polybrene (Sigma-Aldrich; #H9268), doxycycline (Duchefa Biochemie, Haarlem, The Netherlands; #D0121), puromycin (Santa Cruz Biotechnology, Dallas, TX, USA; #sc-108071), blasticidin (Thermo Fisher Scientific, Waltham MA, USA; #R21001), CellTracker Green (Thermo Fisher Scientific; #C7025). BV6 was a kind gift from Genentech.

Cell lines

The human Jurkat T lymphocyte cell line (JA3) and its caspase-9-negative subclone (JA3-C9) were kindly provided by J. Blenis (Harvard Medical School, Boston, MA, USA). Mouse embryonic fibroblasts (MEF) and their caspase-9-deficient counterparts (MEF-C9) were kindly provided by Andreas Strasser (The Walter and Eliza Hall Institute of Medical Research, Australia) [54]. Jurkat and WSU cells were cultured in RPMI-1640 (Sigma-Aldrich; #R5886), MEFs were cultured in Dulbecco's Modified Eagle Medium (DMEM) low glucose (Sigma-Aldrich; #D5546), and HEK293FT cells were cultured in DMEM high glucose (Sigma-Aldrich; #D5796) in a humidified atmosphere of 5% CO_2 at 37 °C, respectively. All media were supplemented with 10 % FBS, 2 mM L-glutamine, and 40 $mg{\cdot}L^{-1}$ gentamicin.

Measurement of cell viability

A total of 5×10^5 cells were pretreated with the indicated reagents: 10–50 μM Z-VAD, 1 μM BV6, 0.4 $\mu g{\cdot}mL^{-1}$ CHX, 2.5 μM CCT137690, 20 μM AR-A014418, 40 μM Nec-1, or 1 μM NSA for 1 h and activated with the indicated stimuli for 24 h: 30 $ng{\cdot}mL^{-1}$ flag-tagged recombinant FasL cross-linked with the anti-FLAG M2 antibody (Sigma-Aldrich; #F1804), 50 $ng{\cdot}mL^{-1}$ human TNF-α, 40 $ng{\cdot}mL^{-1}$ flag-tagged recombinant Trail cross-linked with the anti-FLAG M2 antibody, 400 μM H_2O_2, 0.74–6.7 μM ionomycin, 100 $ng{\cdot}mL^{-1}$ LPS or cocultured with cell tracker green-stained human FasL expressing WSU B cells or infected with HHV-1 (ATCC-VR-1493) at MOI 5.

To distinguish between Jurkat and WSU-FasL cells, WSU-FasL was stained using CellTracker™ Green CMFDA Dye. Cells were loaded with 10 $ng{\cdot}mL^{-1}$ CellTracker at 37 °C for 30 min. After washing, 2.5×10^6 cells in 0.5 mL volume were cocultured with 5×10^5 unlabeled Jurkat cells in 24-well tissue culture plates. Cell death was determined after 24 h by propidium iodide (PI, Sigma-Aldrich) staining (10 $\mu g{\cdot}mL^{-1}$) only in the cell tracker-negative population. Cell death was measured by flow cytometry using BD FACSCalibur™ flow cytometer (BD Biosciences, San Jose, CA, USA), and data were analyzed by FLOWJO software (Tree Star, Ashland, OR, USA).

CCK8 assay

A total of 2×10^4 Jurkat cells were treated with either 1.25–80 μM CCT137690 or 10–640 μM AR-A014418 for 24 h in a 96-well plate. Cell cytotoxicity was measured with Cell Counting Kit-8 (ApexBio; #K1018) according to the manufacturer's protocol. Briefly, 10 μL CCK-8 solution was added to each well and then incubated for 4 h. Absorbance was measured with EnVision® 2105 multimode plate reader (PerkinElmer, Waltham, MA, USA) at 450 nm. All experiments were performed in quadruplicate, and cell viability (%) was expressed as a percentage relative to the untreated control cells.

Caspase activity assay

We used Apo-ONE Homogeneous Caspase-3/7 Assay (Promega, Madison, WI, USA; #G7792) to evaluate the activity of caspase-3 and caspase-7, respectively. Jurkat cells ($2x10^4$) were pretreated with 10 μM Z-VAD, 1 μM BV6, and 40 μM Nec-1 for 1 h and activated for 24 h with 50 $ng{\cdot}mL^{-1}$ human TNF-α in 96-well black tissue culture plates (SPL Life Sciences, Pocheon-si, Korea; #31296). The reactions to detect caspase-3/7 activity were performed following the manufacturer's protocol. Fluorescence was measured using Synergy HT Multimode Microplate Reader configured to detect caspase-3/7 activity at an excitation wavelength range of 485 ± 20 nm and an emission wavelength range of 528 ± 20 nm.

Western blotting

Protein extraction was performed by lysing the cells in 2× Laemmli sample buffer (4% SDS, 20% glycerol, 10% 2-mercaptoethanol, 0.004% bromophenol blue, 0.125 M Tris/HCl, pH 6.8). Proteins were separated by SDS gel electrophoresis using 10% polyacrylamide gels and transferred

onto nitrocellulose membranes (Bio-Rad Laboratories, Hercules, CA, USA; #1620115). Nonspecific binding was blocked by TBS-Tween with 5% nonfat dry milk. Transfer membranes were immunoblotted with the indicated antibodies: caspase-9 (MBL Life science, Tokyo, Japan; #M054-3), caspase-8 (Cell Signaling Technology, Danvers, MA, USA; #9746S), RIPK1 (BD Biosciences; #610459), RIPK3 (Cell Signaling Technology; #13526), GSK3ß (Cell Signaling Technology; #9315), Aurora A (Cell Signaling Technology; #14475), TAK1 (Cell Signaling Technology; #5206S), CYLD (Sigma-Aldrich; #SAB4200060), pRIPK1 (Cell Signaling Technology; #65746), pRIPK3 (Abcam; #ab209384), phospho-Aurora A (Thr288) (Cell Signaling Technology; #2914), and β-actin (Santa Cruz Biotechnology; #sc-47778) all diluted 1 : 1000. Anti-rabbit (GE Healthcare, Chicago, IL, USA; #NA934), anti-mouse (GE Healthcare; #NA931) antibodies or anti-rat (Sigma-Aldrich; #A9037) antibodies conjugated to horseradish peroxidase were used as secondary antibodies in the dilution of 1 : 5000. For mouse cells, the following mouse-specific antibodies were used: caspase-8 (Cell Signaling Technology; #4927S), phospho-RIP (Ser166) antibody (Rodent Specific) (Cell Signaling Technology; #31122), phospho-RIP3 (Thr231/Ser232) (Cell Signaling Technology; #91702).

Immunoprecipitation

A total of $5x10^7$ Jurkat cells were pretreated with 10 μM Z-VAD and 1 μM BV6 for 1 h and activated for the indicated times with 50 ng·mL^{-1} human TNF-α. Cells were lysed using 1% Triton X-100 with protease inhibitor (Sigma-Aldrich; #P8340) and phosphatase inhibitor (Sigma-Aldrich; #P2850) in lysis buffer (30 mM Tris, 140 mM NaCl, 5 mM EDTA, 1 mM Na_3VO_4, 50 mM NaF, 2 mM $Na_4P_2O_7$, pH 7.6). Protein concentration was determined using Pierce™ BCA Protein Assay Kit (Thermo Fisher Scientific; #23227). Equal amounts of total protein were added to protein A/G PLUS-agarose beads (Santa Cruz Biotechnology; #sc-2003) precoated with the indicated antibodies: caspase-9 (LifeSpan BioSciences, Seattle, WA, USA; #LS-C148248), RIPK1 (BD Biosciences; #610459), and RIPK3 (Cell Signaling Technology; #13526). The content was gently rotated at 4 °C overnight. The next day, the beads were washed four times with lysis buffer on ice and then subjected to western blotting analysis. Anti-rabbit light chain (Merck Millipore, Burlington, MA, USA; #MAB201) or anti-mouse light chain (Merck Millipore; #AP200P) antibodies conjugated to horseradish peroxidase were used as the secondary antibodies in the dilution of 1 : 5000.

Plasmids and constructs

To generate the lentivector expressing RIPK1, pCR3-FLAGhRIP1 (#LMBP 4850) was purchased from CABRI, for RIPK3, hRIP3 GFP wt was a gift from Francis Chan (Addgene plasmid #41387) [51], and for caspase-9, pET23b-Casp9-His was a gift from Guy Salvesen (Addgene plasmid #11829) [55]. RIPK1, RIPK3, and caspase-9 were first cloned into pENTR4-FLAG provided by Eric Campeau & Paul Kaufman (Addgene plasmid #17423) [56]. RIPK1 and RIPK3 were further subcloned into the all-in-one doxycycline-inducible lentiviral destination vector, pCW57.1 (a gift from David Root, Addgene plasmid #41393), while caspase-9 was subcloned into pLenti CMV Blast DEST (a gift from Eric Campeau & Paul Kaufman, Addgene plasmid #17451) [56] and used for lentiviral transduction of wild-type Jurkat cells (RIPK1 JA3 and RIPK3 JA3), and their caspase-9-deficient counterparts (RIPK1 JA3-C9 and RIPK3 JA3-C9, JA3-C9 retr). All cloning was checked by restriction analysis and DNA sequencing (capillary sequencing runs were performed by UD-GenoMed Medical Genomic Technologies Ltd.).

Lentivirus production and transduction

Replication-deficient lentivirus used in the gene transfer experiments was created as previously described [57]. Briefly, 22 μg pCW57.1-RIPK1, pCW57.1-RIPK3, or pLENTI-Casp9 lentiviral backbone vector together with 15 μg pMD2.G and 5 μg psPAX2 were combined together in a 50-mL centrifuge tube. pMD2.G (Addgene #12259) and psPAX2 (Addgene #12260) were a gift from Didier Trono. Calcium phosphate precipitation was performed by adding 1.35 mL distilled H_2O and 150 μL 2.5 M $CaCl_2$ and 1.5 mL 2× HEPES-buffered saline (280 mM NaCl, 50 mM HEPES, 1.5 mM Na_2HPO_4, pH 7.0) was added dropwise into the centrifuge tube under constant agitation. The solution was incubated at room temperature for 30 min and then added dropwise to HEK293FT cells grown in T75 cell culture flask. 16 h post-transfection, the medium was replaced with fresh DMEM high glucose (Sigma-Aldrich; #D5796) supplemented with 10 % FBS, 2 mM L-glutamine. Viral supernatants were collected at 48- and 72-h post-transfection and passed through a 0.45-μm filter. Target cells were incubated overnight with lentiviral supernatant in the presence of 4 μg·mL^{-1} polybrene. Infected cells were selected with 5 μg·mL^{-1} puromycin or 10 μg·mL^{-1} blasticidin for 7 days.

Generation of caspase-9 conditional KO mice

CRISPR/Cas9 technology was used to insert loxP sites into the introns harboring the second exon of the caspase-9 gene. Guide RNAs targeting the intronic sequences were synthetized *in vitro*. The DNA templates carrying the loxP sequences and the homology arms for homology-directed repair were synthetized as single-stranded ultramer oligonucleotides (ssODN, from IDT). The two guide RNAs, the two ssODNs, and a Cas9 mRNA (Trilink) were coinjected into the pronuclei of fertilized eggs of FVB/Ant mice. Genotyping was carried out with a PCR-based strategy to detect size

differences after insertion. After it was confirmed that both loxP sites integrated on the same allele, the modification was sequence verified. FVB/Ant mice with loxP sites were backcrossed with C57BL/6J for eight generations.

To achieve pancreatic acinar cell-specific caspase-9 knockout, LoxP animals were crossed with mice expressing tamoxifen-inducible Cre recombinase under the regulation of the Cela1 promoter in pancreatic acinar cells (Jackson Laboratory, Tg(Cela1-cre/ERT)1Lgdn/J; Stock No:025736). Mice homozygous for LoxP and hemizygous for Cre recombinase were used in the experiments. Activation of the Cre recombinase was achieved by tamoxifen administration (5 mg·mL^{-1} in sunflower oil, 125 mg/bwkg) in oral gavage for five consecutive days. All mice were housed in SPF facilities at 21 °C and 31% humidity. All mice were maintained under general housing environment, fed sterilized food, and autoclaved water *ad libitum*. Experiments on live animals were carried out with adherence to the NIH guidelines and the EU directive 2010/63/EU for the protection of animals used for scientific purposes. The study was authorized by the National Scientific Ethical Committee on Animal Experimentation under license number XXI./1542/2020.

Acute pancreatitis model

Experimental AP was induced as described previously [58]. Briefly, mice received eight hourly i.p. injections of 50 μg/bwkg cerulein (Bachem, Bubendorf, Switzerland; #H-3220) and were sacrificed 12 h after the induction of AP (n = 6-8, 8-week-old mice per group). All animals were randomly divided into the control and treated groups, No specific exclusion criteria were applied. Blood and tissue samples were collected after terminal anesthesia immediately. Blood samples were centrifuged at 2500 RCF for 15 min at 4 °C, and serums were stored at −20 °C. Pieces of pancreatic tissue were placed into a 4% formaldehyde solution and stored at 4 °C until histology. Serum amylase activity was measured by a colorimetric kit (Diagnosticum Zrt., Budapest, Hungary; #47462) according to the manufacturer's instruction, and absorbance was detected at 405 nm using a FLUOstar OPTIMA (BMG Labtech, Ortenberg, Germany) microplate reader. For routine histology, formaldehyde-fixed pancreas samples were embedded in paraffin, and 4 μm thick sections were stained with hematoxylin–eosin. Histological scores for edema, inflammatory cell infiltration, and necrosis were evaluated by three independent investigators blinded to the protocol (0–5 points for edema, leukocyte infiltration, and % of the total area for necrosis) [59].

Immunofluorescent labeling

For verification of conditional knockout of caspase-9 in pancreatic acinar cells, a monoclonal caspase-9 antibody was used. Whole pancreatic tissue samples were frozen in Shandon Cryomatrix (Thermo Fisher Scientific; #6769006), and 7 μm thick sections were cut with a cryostat (Leica CM 1860 UV; Leica, Wetzlar, Germany). Antibody labeling was performed as previously described [60]. Sections were fixed in 4% PFA-PBS and after antigen retrieval and blocking, were incubated with anti-caspase-9 (Abcam; #ab202068) primary rabbit monoclonal antibody overnight at 4 °C (1 : 100 dilution). Secondary antibody labeling was performed with a goat anti-rabbit IgG secondary antibody conjugated with Alexa Fluor 488 (Thermo Fisher Scientific; #A-11034). Nuclei were stained with Hoechst-33342, and sections were covered with Fluoromount mounting medium (Sigma-Aldrich; #F4680). Images were captured with a Zeiss LSM880 confocal microscope with a 40× oil immersion objective (Carl Zeiss Microscopy GmbH, Jena, Germany, NA: 1.4).

Total protein isolation from whole pancreatic tissue

Whole mouse pancreatic tissue was cut to small pieces with a razor blade and resolved in 1 mL RIPA lysis buffer (Merck Millipore; #20-188) completed with EASYpack Protease Inhibitor Cocktail (Roche, Basel, Switzerland; #05892970001). Branson Sonifier SFX150 (Branson Ultrasonics Corporation, Danbury, CT, USA) was used for the tissue homogenization, during which samples were kept on ice. After the tissue disruption, samples were centrifuged at 1500 ***g*** for 10 min on 4 °C. Finally, supernatant was frozen by the 'snap-freeze' method. Samples were stored at −80 °C until use.

Statistical analysis

Two-way ANOVA or one-way ANOVA, followed by Sidak's multiple comparisons test, was used for multiple comparisons. Results are expressed as mean ± SD. The results are expressed as mean + SD. All analyses were performed by using GRAPHPAD PRISM software (GraphPad Software, Inc., San Diego, CA, USA), version 6.0. Differences were considered to be statistically significant at $P < 0.05$. Significance is indicated by $*P < 0.05$; $**P < 0.01$; $***P < 0.005$; $****P < 0.001$.

Acknowledgements

We thank Zsuzsanna Debreceni and Jerome Durivault for their excellent technical assistance. The JA3 Jurkat cell line and its caspase-9-negative subclones were kindly provided by John Blenis. Caspase-9-deficient MEF cell line was a kind gift of Andreass Strasser and Vanessa Solomon. BV6 was kindly provided by Genentech. Capillary sequencing runs were performed by UD-GenoMed Medical Genomic Technologies Ltd.

The European Regional Development Fund GINOP-2.3.2-15-2016-00050 and the National

Research, Development and Innovation Office—NKFIH 125224 are acknowledged for financial support of this work. M.T. was supported by the ÚNKP-20-4 New National Excellence Program of the Ministry for Innovation and Technology from the source of the National Research Development and Innovation Fund and by the EFOP-3.6.3-VEKOP-16-2017-00009 project cofinanced by EU and the European Social Fund. J.M. was founded by the Hungarian Academy of Sciences (LP2017–18/2017) and by the National Excellence Programme (20391-3/2018/FEKUSTRAT). L.V. received funding from the National Research, Development and Innovation Office grants GINOP-2.3.2-15-2016-00020 TUMORDNS, GINOP-2.3.2-15-2016-00048-STAYALIVE, OTKA K132193. R.K. was supported by the Janos Bolyai Research Fellowship of the Hungarian Academy of Science and by the ÚNKP-19-4 New National Excellence Program of the Ministry of Innovation and Technology and received grant support from NKFIH 129139. A.P-Sz. was supported by the GINOP-2.3.2-15-2016-00032.

Conflict of interest

The authors declare no conflict of interest.

Author contributions

TM, RK, ZSV, PG, and APSz performed experiments, analyzed, and interpreted the data. ECs investigated the effect of HSV1 LV, ZM, FE, and GSZ generated the caspase-9 floxed mouse line. PP, BT, and JM performed *in vivo* pancreatitis model. LV, AOH, JM, AB, and GK provided financial support. GK conceptualized, and TM, LV, AB, JM, and GK wrote and reviewed the manuscript. All authors revised the manuscript and approved the final version of the manuscript.

Peer Review

The peer review history for this article is available at https://publons.com/publon/10.1111/febs.15898.

References

1 Galluzzi L, Vitale I, Aaronson SA, Abrams JM, Adam D, Agostinis P, Alnemri ES, Altucci L, Amelio I, Andrews DW *et al.* (2018) Molecular mechanisms of cell death: recommendations of the Nomenclature Committee on Cell Death 2018. *Cell Death Differ* **25**, 486–541.

2 Holler N, Zaru R, Micheau O, Thome M, Attinger A, Valitutti S, Bodmer JL, Schneider P, Seed B & Tschopp J (2000) Fas triggers an alternative, caspase-8-independent cell death pathway using the kinase RIP as effector molecule. *Nat Immunol* **1**, 489–495.

3 Schutze S, Tchikov V & Schneider-Brachert W (2008) Regulation of TNFR1 and CD95 signalling by receptor compartmentalization. *Nat Rev Mol Cell Biol* **9**, 655–662.

4 Wajant H (2002) The Fas signaling pathway: more than a paradigm. *Science* **296**, 1635–1636.

5 Barnhart BC, Alappat EC & Peter ME (2003) The CD95 type I/Type II model. *Semin Immunol* **15**, 185–193.

6 Schulze-Osthoff K, Ferrari D, Los M, Wesselborg S & Peter ME (1998) Apoptosis signaling by death receptors. *Eur J Biochem* **254**, 439–459.

7 Kroemer G, Galluzzi L & Brenner C (2007) Mitochondrial membrane permeabilization in cell death. *Physiol Rev* **87**, 99–163.

8 Li P, Nijhawan D, Budihardjo I, Srinivasula SM, Ahmad M, Alnemri ES & Wang X (1997) Cytochrome c and dATP-dependent formation of Apaf-1/caspase-9 complex initiates an apoptotic protease cascade. *Cell* **91**, 479–489.

9 Li Y, Zhou M, Hu Q, Bai XC, Huang W, Scheres SH & Shi Y (2017) Mechanistic insights into caspase-9 activation by the structure of the apoptosome holoenzyme. *Proc Natl Acad Sci USA* **114**, 1542–1547.

10 Wu CC, Lee S, Malladi S, Chen MD, Mastrandrea NJ, Zhang Z & Bratton SB (2016) The Apaf-1 apoptosome induces formation of caspase-9 homo- and heterodimers with distinct activities. *Nat Commun* **7**, 13565.

11 Han J, Zhong CQ & Zhang DW (2011) Programmed necrosis: backup to and competitor with apoptosis in the immune system. *Nat Immunol* **12**, 1143–1149.

12 Vandenabeele P, Declercq W, Van Herreweghe F & Vanden Berghe T (2010) The role of the kinases RIP1 and RIP3 in TNF-induced necrosis. *Sci Signal* **3**, re4.

13 Degterev A, Huang Z, Boyce M, Li Y, Jagtap P, Mizushima N, Cuny GD, Mitchison TJ, Moskowitz MA & Yuan J (2005) Chemical inhibitor of nonapoptotic cell death with therapeutic potential for ischemic brain injury. *Nat Chem Biol* **1**, 112–119.

14 He S, Wang L, Miao L, Wang T, Du F, Zhao L & Wang X (2009) Receptor interacting protein kinase-3 determines cellular necrotic response to TNF-alpha. *Cell* **137**, 1100–1111.

15 Zhao J, Jitkaew S, Cai Z, Choksi S, Li Q, Luo J & Liu Z-G (2012) Mixed lineage kinase domain-like is a key receptor interacting protein 3 downstream component of TNF-induced necrosis. *Proc Natl Acad Sci USA* **109**, 5322–5327.

16 Vercammen D, Beyaert R, Denecker G, Goossens V, Van Loo G, Declercq W, Grooten J, Fiers W & Vandenabeele P (1998) Inhibition of caspases increases

the sensitivity of L929 cells to necrosis mediated by tumor necrosis factor. *J Exp Med* **187**, 1477–1485.
17 Lin Y, Devin A, Rodriguez Y & Liu ZG (1999) Cleavage of the death domain kinase RIP by caspase-8 prompts TNF-induced apoptosis. *Genes Dev* **13**, 2514–2526.
18 Vanden Berghe T, Kaiser WJ, Bertrand MJ & Vandenabeele P (2015) Molecular crosstalk between apoptosis, necroptosis, and survival signaling. *Mol Cell Oncol* **2**, e975093.
19 Ch'en IL, Tsau JS, Molkentin JD, Komatsu M & Hedrick SM (2011) Mechanisms of necroptosis in T cells. *J Exp Med* **208**, 633–641.
20 O'Donnell MA, Perez-Jimenez E, Oberst A, Ng A, Massoumi R, Xavier R, Green DR & Ting AT (2011) Caspase 8 inhibits programmed necrosis by processing CYLD. *Nat Cell Biol* **13**, 1437–1442.
21 Molnar T, Mazlo A, Tslaf V, Szollosi AG, Emri G & Koncz G (2019) Current translational potential and underlying molecular mechanisms of necroptosis. *Cell Death Dis* **10**, 860.
22 Jouan-Lanhouet S, Riquet F, Duprez L, Vanden Berghe T, Takahashi N & Vandenabeele P (2014) Necroptosis, *in vivo* detection in experimental disease models. *Semin Cell Dev Biol* **35**, 2–13.
23 Christofferson DE & Yuan J (2010) Necroptosis as an alternative form of programmed cell death. *Curr Opin Cell Biol* **22**, 263–268.
24 Wang G, Qu FZ, Li L, Lv JC & Sun B (2016) Necroptosis: a potential, promising target and switch in acute pancreatitis. *Apoptosis* **21**, 121–129.
25 Xie Y, Zhu S, Zhong M, Yang M, Sun X, Liu J, Kroemer G, Lotze M, Zeh HJ 3rd, Kang R & *et al.* (2017) Inhibition of aurora kinase A induces necroptosis in pancreatic carcinoma. *Gastroenterology* **153**, 1429–1443.e5.
26 Li D, Xu T, Cao Y, Wang H, Li L, Chen S, Wang X & Shen Z (2015) A cytosolic heat shock protein 90 and cochaperone CDC37 complex is required for RIP3 activation during necroptosis. *Proc Natl Acad Sci USA* **112**, 5017–5022.
27 Zhao XM, Chen Z, Zhao JB, Zhang PP, Pu YF, Jiang SH, Hou JJ, Cui YM, Jia XL & Zhang SQ (2016) Hsp90 modulates the stability of MLKL and is required for TNF-induced necroptosis. *Cell Death Dis* **7**, e2089.
28 Chen W, Wu J, Li L, Zhang Z, Ren J, Liang Y, Chen F, Yang C, Zhou Z, Su SS *et al.* (2015) Ppm1b negatively regulates necroptosis through dephosphorylating Rip3. *Nat Cell Biol* **17**, 434–444.
29 Duprez L, Takahashi N, Van Hauwermeiren F, Vandendriessche B, Goossens V, Vanden Berghe T, Declercq W, Libert C, Cauwels A & Vandenabeele P (2011) RIP kinase-dependent necrosis drives lethal systemic inflammatory response syndrome. *Immunity* **35**, 908–918.
30 Yoon S, Bogdanov K, Kovalenko A & Wallach D (2016) Necroptosis is preceded by nuclear translocation of the signaling proteins that induce it. *Cell Death Differ* **23**, 253–260.
31 Murai S, Yamaguchi Y, Shirasaki Y, Yamagishi M, Shindo R, Hildebrand JM, Miura R, Nakabayashi O, Totsuka M, Tomida T *et al.* (2018) A FRET biosensor for necroptosis uncovers two different modes of the release of DAMPs. *Nat Commun* **9**, 4457.
32 Shi G, Jia P, Chen H, Bao L, Feng F & Tang H (2018) Necroptosis occurs in osteoblasts during tumor necrosis factor-alpha stimulation and caspase-8 inhibition. *Braz J Med Biol Res* **52**, e7844.
33 Saito Y, Nishio K, Ogawa Y, Kimata J, Kinumi T, Yoshida Y, Noguchi N & Niki E (2006) Turning point in apoptosis/necrosis induced by hydrogen peroxide. *Free Rad Res* **40**, 619–630.
34 Feoktistova M, Geserick P, Kellert B, Dimitrova DP, Langlais C, Hupe M, Cain K, MacFarlane M, Hacker G & Leverkus M (2011) cIAPs block Ripoptosome formation, a RIP1/caspase-8 containing intracellular cell death complex differentially regulated by cFLIP isoforms. *Mol Cell* **43**, 449–463.
35 Petersen SL, Wang L, Yalcin-Chin A, Li L, Peyton M, Minna J, Harran P & Wang X (2007) Autocrine TNFalpha signaling renders human cancer cells susceptible to Smac-mimetic-induced apoptosis. *Cancer Cell* **12**, 445–456.
36 Sridharan H & Upton JW (2014) Programmed necrosis in microbial pathogenesis. *Trends Microbiol* **22**, 199–207.
37 Huang Z, Wu SQ, Liang Y, Zhou X, Chen W, Li L, Wu J, Zhuang Q, Chen C, Li J *et al.* (2015) RIP1/RIP3 binding to HSV-1 ICP6 initiates necroptosis to restrict virus propagation in mice. *Cell Host Microbe* **17**, 229–242.
38 Galluzzi L, Bravo-San Pedro JM, Vitale I, Aaronson SA, Abrams JM, Adam D, Alnemri ES, Altucci L, Andrews D, Annicchiarico-Petruzzelli M *et al.* (2015) Essential versus accessory aspects of cell death: recommendations of the NCCD. *Cell Death Differ* **22**, 58–73.
39 Sperandio S, de Belle I & Bredesen DE (2000) An alternative, nonapoptotic form of programmed cell death. *Proc Natl Acad Sci USA* **97**, 14376–14381.
40 Jager R & Zwacka RM (2010) The enigmatic roles of caspases in tumor development. *Cancers* **2**, 1952–1979.
41 Han J, Hou W, Goldstein LA, Stolz DB, Watkins SC & Rabinowich H (2014) A Complex between Atg7 and Caspase-9: a novel mechanism of cross-regulation between autophagy and apoptosis. *J Biol Chem* **289**, 6485–6497.
42 An HK, Chung KM, Park H, Hong J, Gim JE, Choi H, Lee YW, Choi J, Mun JY & Yu SW (2019) CASP9 (caspase 9) is essential for autophagosome maturation

through regulation of mitochondrial homeostasis. *Autophagy* **16**, 1598–1617.
43 Samraj AK, Keil E, Ueffing N, Schulze-Osthoff K & Schmitz I (2006) Loss of caspase-9 provides genetic evidence for the type I/II concept of CD95-mediated apoptosis. *J Biol Chem* **281**, 29652–29659.
44 Koncz G, Hancz A, Chakrabandhu K, Gogolak P, Kerekes K, Rajnavolgyi E & Hueber AO (2012) Vesicles released by activated T cells induce both Fas-mediated RIP-dependent apoptotic and Fas-independent nonapoptotic cell deaths. *J Immunol* **189**, 2815–2823.
45 McComb S, Shutinoski B, Thurston S, Cessford E, Kumar K & Sad S (2014) Cathepsins limit macrophage necroptosis through cleavage of Rip1 kinase. *J Immunol* **192**, 5671–5678.
46 Guo R, Lin B, Pan JF, Liong EC, Xu AM, Youdim M, Fung ML, So KF & Tipoe GL (2016) Inhibition of caspase-9 aggravates acute liver injury through suppression of cytoprotective autophagy. *Sci Rep* **6**, 32447.
47 Wu J, Huang Z, Ren J, Zhang Z, He P, Li Y, Ma J, Chen W, Zhang Y, Zhou X *et al.* (2013) Mlkl knockout mice demonstrate the indispensable role of Mlkl in necroptosis. *Cell Res* **23**, 994–1006.
48 Louhimo J, Steer ML & Perides G (2016) Necroptosis is an important severity determinant and potential therapeutic target in experimental severe pancreatitis. *Cell Mo Gastroenterol Hepatol* **2**, 519–535.
49 Mareninova OA, Sung KF, Hong P, Lugea A, Pandol SJ, Gukovsky I & Gukovskaya AS (2006) Cell death in pancreatitis: caspases protect from necrotizing pancreatitis. *J Biol Chem* **281**, 3370–3381.
50 Orozco S, Yatim N, Werner MR, Tran H, Gunja SY, Tait SW, Albert ML, Green DR & Oberst A (2014) RIPK1 both positively and negatively regulates RIPK3 oligomerization and necroptosis. *Cell Death Differ* **21**, 1511–1521.
51 Cho YS, Challa S, Moquin D, Genga R, Ray TD, Guildford M & Chan FK (2009) Phosphorylation-driven assembly of the RIP1-RIP3 complex regulates programmed necrosis and virus-induced inflammation. *Cell* **137**, 1112–1123.
52 Zhang DW, Shao J, Lin J, Zhang N, Lu BJ, Lin SC, Dong MQ & Han J (2009) RIP3, an energy metabolism regulator that switches TNF-induced cell death from apoptosis to necrosis. *Science* **325**, 332–336.
53 Wang Q, Liu Z, Ren J, Morgan S, Assa C & Liu B (2015) Receptor-interacting protein kinase 3 contributes to abdominal aortic aneurysms via smooth muscle cell necrosis and inflammation. *Circ Res* **116**, 600–611.
54 Marsden VS, O'Connor L, O'Reilly LA, Silke J, Metcalf D, Ekert PG, Huang DC, Cecconi F, Kuida K, Tomaselli KJ *et al.* (2002) Apoptosis initiated by Bcl-2-regulated caspase activation independently of the cytochrome c/Apaf-1/caspase-9 apoptosome. *Nature* **419**, 634–637.
55 Stennicke HR, Deveraux QL, Humke EW, Reed JC, Dixit VM & Salvesen GS (1999) Caspase-9 can be activated without proteolytic processing. *J Biol Chem* **274**, 8359–8362.
56 Campeau E, Ruhl VE, Rodier F, Smith CL, Rahmberg BL, Fuss JO, Campisi J, Yaswen P, Cooper PK & Kaufman PD (2009) A versatile viral system for expression and depletion of proteins in mammalian cells. *PLoS One* **4**, e6529.
57 Cribbs AP, Kennedy A, Gregory B & Brennan FM (2013) Simplified production and concentration of lentiviral vectors to achieve high transduction in primary human T cells. *BMC Biotechnol* **13**, 98.
58 Maleth J, Balazs A, Pallagi P, Balla Z, Kui B, Katona M, Judak L, Nemeth I, Kemeny LV, Rakonczay Z Jr *et al.* (2015) Alcohol disrupts levels and function of the cystic fibrosis transmembrane conductance regulator to promote development of pancreatitis. *Gastroenterology* **148**, 427–439, e16.
59 Pallagi P, Balla Z, Singh AK, Dosa S, Ivanyi B, Kukor Z, Toth A, Riederer B, Liu Y, Engelhardt R *et al.* (2014) The role of pancreatic ductal secretion in protection against acute pancreatitis in mice*. *Crit Care Med* **42**, e177–e188.
60 Molnar R, Madacsy T, Varga A, Nemeth M, Katona X, Gorog M, Molnar B, Fanczal J, Rakonczay Z Jr, Hegyi P *et al.* (2020) Mouse pancreatic ductal organoid culture as a relevant model to study exocrine pancreatic ion secretion. *Lab Invest* **100**, 84–97.